Int. J. Multiphase Flow Vol. 5, pp. 437–462

0301-9322/79/1201-0437/$02.00/0

EFFECTS OF FLUID PROPERTIES AND PIPE DIAMETER ON TWO-PHASE FLOW PATTERNS IN HORIZONTAL LINES

J. WEISMAN, D. DUNCAN,† J. GIBSON‡ and T. CRAWFORD§

University of Cincinnati, OH 45221, U.S.A.

(*Received* 5 *December* 1978; *in revised form* 18 *June* 1979)

Abstract—Extensive new data have been obtained on the transitions between two-phase flow patterns during co-current gas liquid flow in horizontal lines. Fluid properties were varied in a systematic manner to determine the effects of liquid viscosity, liquid density, interfacial tension and gas density. Line sizes varied from 1.2 to 5 cm for most of the tests. Visual observations were supplemented by an analysis of pressure drop fluctuations and hence the present data are believed to be less subjective than most past observations.

The transition data from the present tests, as well as available literature data, were compared to the most frequently used transition line correlations. In almost all cases serious deficiencies were observed. Revised dimensionless correlations which fit present data, and those previously available, are presented.

INTRODUCTION

Two phase flow patterns in horizontal pipelines have been experimentally studied by a number of investigators (Alves 1954; Bergelin & Gazley 1949; Eaton *et al.* 1967; Govier & Omer 1962; Hoogendorn & Beutelaar 1961; Kosterin 1962; Sekoguchi *et al.* 1973; Schicht 1969; and White & Huntington 1955). However, most of these studies were confined to the air–water system. Eaton *et al.* (1967) examined several systems with varying fluid properties but their flow pattern definitions were different than those commonly used. Further, they reported their data in terms of a flow map which requires a knowledge of the void fraction. Their data are therefore difficult to interpret and use. Hoogendorn *et al.* (1959, 1961) did investigate several fluid systems and did report their data in a usable manner. However, fluid properties were not varied in any systematic way and it is difficult to determine the effects of individual properties on the transitions between flow patterns. Further, for some fluid systems investigated, data were obtained only over relatively limited velocity ranges.

This study was designed to obtain reliable data on the effect of fluid properties and pipe diameter on flow pattern transitions in horizontal pipe lines over wide velocity ranges. The fluids chosen for the experiments were selected so as to allow large changes in one property while producing only relatively unimportant changes in other properties. Visual observations of flow patterns were supplemented by observations of the fluctuation in pressure drop between two taps a short distance apart. These pressure drop fluctuations were found to be characteristic of the flow pattern present.

EXPERIMENTAL APPARATUS

The major portion of the data obtained in this investigation was obtained with a large loop designed for operation with air and aqueous solutions. The loop constructed for these experiments is shown schematically in figure 1. Liquid from the separator tank (K) is pumped by the centrifugal pump (A) to the test section (F) or is recirculated through the cooler (Q) back to the pump inlet. The flow split is determined by the relative positions of valves (B) and (R). The recirculation line generally carries more than 50% of the pump output and provides stable operation in two-phase flow. Liquid flow to the test section is measured by the orifice meter tube section (C). Valves (D) control the liquid flow to the test section.

†Present address: General Electric Company, Schnectady, New York.
‡Present address: Combustion Engineering, Windsor, Connecticut.
§Present address: Philadelphia Electric, Philadelphia, Pennsylvania.

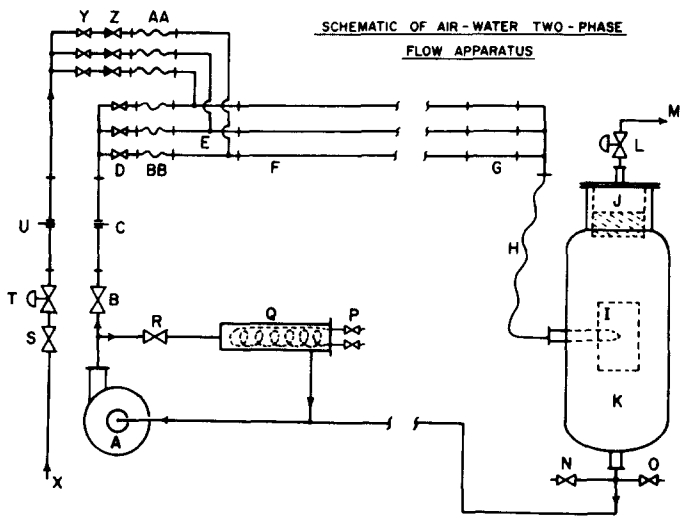

Figure 1. Air–water loop.

Air is obtained from a large compressor located below the loop area. The pressure of air from the supply (X) is regulated by valve (T). The air flow rate is measured by the orifice meter-tube section (U) and the air flow rate into the test section is controlled by valves (Y). Back flow of liquid into the air lines is prevented by check valves (Z). Mixing of air and liquid phases is accomplished at horizontal tees (E).

Flexible hose (H) leads from the test section to the separator tank (K) where a centrally located centrifugal separator (I) performs the primary separation of the air and liquid phases. Any water entrained in the air is removed by the demister pad (J). Any small gas bubbles remaining in the liquid rise to the surface is the very low flow region surrounding the centrifugal separator.

The test sections consist of three 6.1 m long sections of glass pipe. The pipes are of 1.2 cm, 2.5 cm and 5.1 cm nominal size i.d. The flexible line to the separating tank allows the test section to be inclined at upward angles up to 10° and downward angles up to about 7°.

Measurement of the tubing used showed the two larger sized has diameters very close to the nominal size. The 1.2 cm size, however, showed some variation in diameter and the actual diameter appeared close to ~ 1.15 cm. This value was used in velocity calculations.

At the end of each glass pipe, two pressure taps were provided. The pressure taps, which are 15 cm apart in a given line, are connected through a manifold to a sensitive strain-gauge differential pressure transducer. The transducer output is recorded on an oscillograph. The pressure transducer was located below all of the test sections and provisions for water purge to the connecting lines was provided. The manifold lines were always purged and filled with water prior to measurement of differential pressures.

Data was also obtained with the boiling freon system shown in figure 2. Freon 113 was circulated at rates up to 114 l./min by a centrifugal pump with specially designed seals. After measurement of the total liquid flow via an orifice, the freon flowed to two vertical heaters where vapor was generated. The mixture then flowed to a 1.52 m long, horizontal 1 in. schedule 80 pipe (i.d. 2.45 cm) which preceded the test section. The test section was 1.52 m long length of 2.54 cm i.d. glass pipe. Care was taken to minimize any discontinuity at the glass–steel pipe interface.

The test section was followed by a capacitance type void sensor and a drag disk with a fine screen in front of it. For most of the flow range, the mass flow of vapor was computed by recognizing that the drag disk signal was proportional to the square of the total mass velocity divided by the density. Previous tests (Weisman 1977) have shown that, when the drag disk was preceded by a fine screen, the fluid density to which the drag disk responded was the homogeneous density (velocity ratio = 1). At the highest flow rates, the pressure drop across the

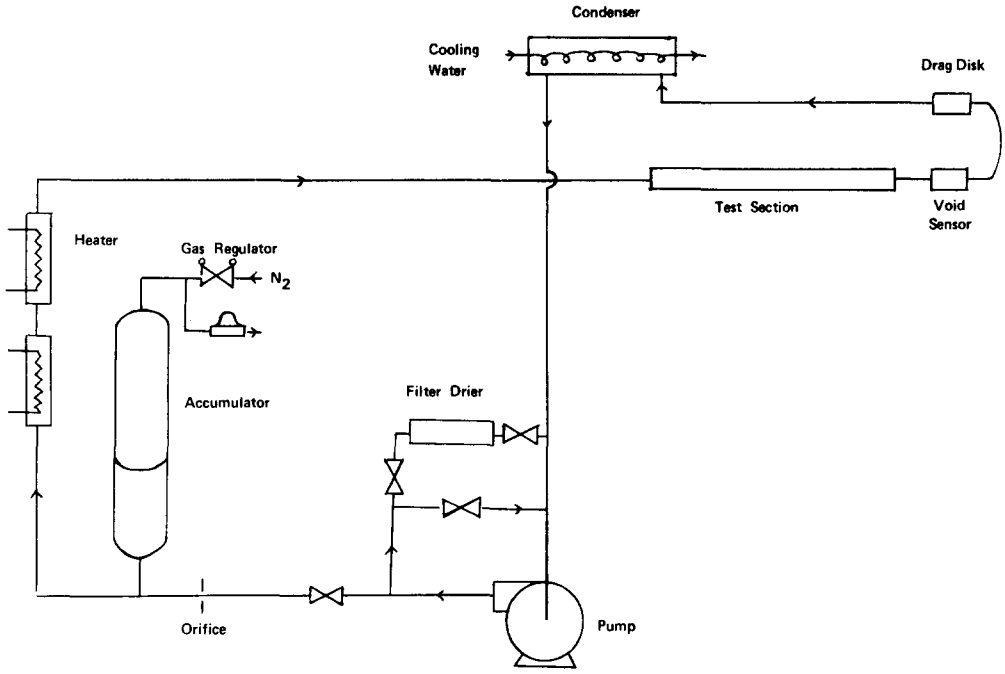

Figure 2. Boiling Freon loop.

drag disk was too high and it had to be removed. The mass flow of vapor was then computed from the measured void fraction and a realistic estimation of the slip ratio in the test section line.

The mixture leaving the drag disk proceeded to a condenser. In addition to condensing all the vapor, the condenser supplied sufficient subcooling to prevent cavitation at the pump inlet.

BASELINE EXPERIMENTS WITH AIR-WATER SYSTEM

Observations of the air-water system indicated that the flow pattern classification of Mandhane *et al.* (1974) provided a good characterization of the visually distinguishable flow patterns. Accordingly, the following classification was used in reporting observations.

(a) Plug, Bubble—elongated bubbles (plugs) or bubbles of gas moving through liquid.

(b) Stratified—quiescent liquid at bottom of tube, gas obove.

(c) Wavy—liquid with wavy surface at bottom of tube, gas above.

(d) Slug—packets of liquid (slugs) periodically moving down tube.

(e) Annular—liquid around outside of tube and gas core (may have suspended droplets) in center.

(f) Dispersed—small bubbles of gas dispersed throughout liquid or small droplets of liquid dispersed throughout gas (mist flow).

Visual criteria were established for each of the flow patterns. Annular flow was distinguished from wavy slug, or dispersed flow by the existence of a continuous liquid film around the entire tube circumference. As the liquid velocity is increased, more and more liquid is entrained within the central gas core. Annular flow was said to have changed to dispersed flow when all of the liquid appeared to have been dispersed and a continuous liquid film was no longer visible. Dispersed flow also described the essentially homogeneous froth seen at high liquid flow rates but low or moderate gas flows. The flow pattern is fairly readily distinguished from slug or plug but in the transition region periodic flow pulsations are still seen. Slug, plug and bubble flow was distinguished from dispersed flow by the existence of gas volumes which remained at the top of the tube. As the liquid flow is reduced, the gas volumes become longer and eventually the liquid bridge between the gas volumes disappears leaving the continuous gas

layer characteristic of stratified and wavy flow. The flow was said to be wavy if there was an observable wave on the free liquid surface. In the flow maps shown subsequently, the transition regions represent the often chaotic region between flow patterns in which it was difficult to determine if a given flow pattern criteria was being met.

In describing and correlating the flow pattern behavior, it is often desirable to make use of Hubbard & Dukler (1966) suggestion for consolidation of these flow patterns. It is convenient to refer to the combined stratified and wavy flow pattern area as "separated" flow and to combine slug and plug as "intermittent" flow.

The first question which was addressed experimentally was whether a sufficient length to diameter (L/D) ratio had been provided so that observations taken at the end of the pipeline could be considered to be representation of an equilibrium situation. Simpson *et al.* (1977) noted that, even with an L/D of 128, some differences could be observed between experiments with the air–water mixer at the beginning of the straight run and experiments with the mixer located before a bend which preceded the straight run. The differences he observed were small except for the separated-intermittent transition.

In the present tests, observations were taken at the end of each pipe-line, the middle of the pipeline and approx. 8 in. from the simple horizontal tee used as a mixing device. The

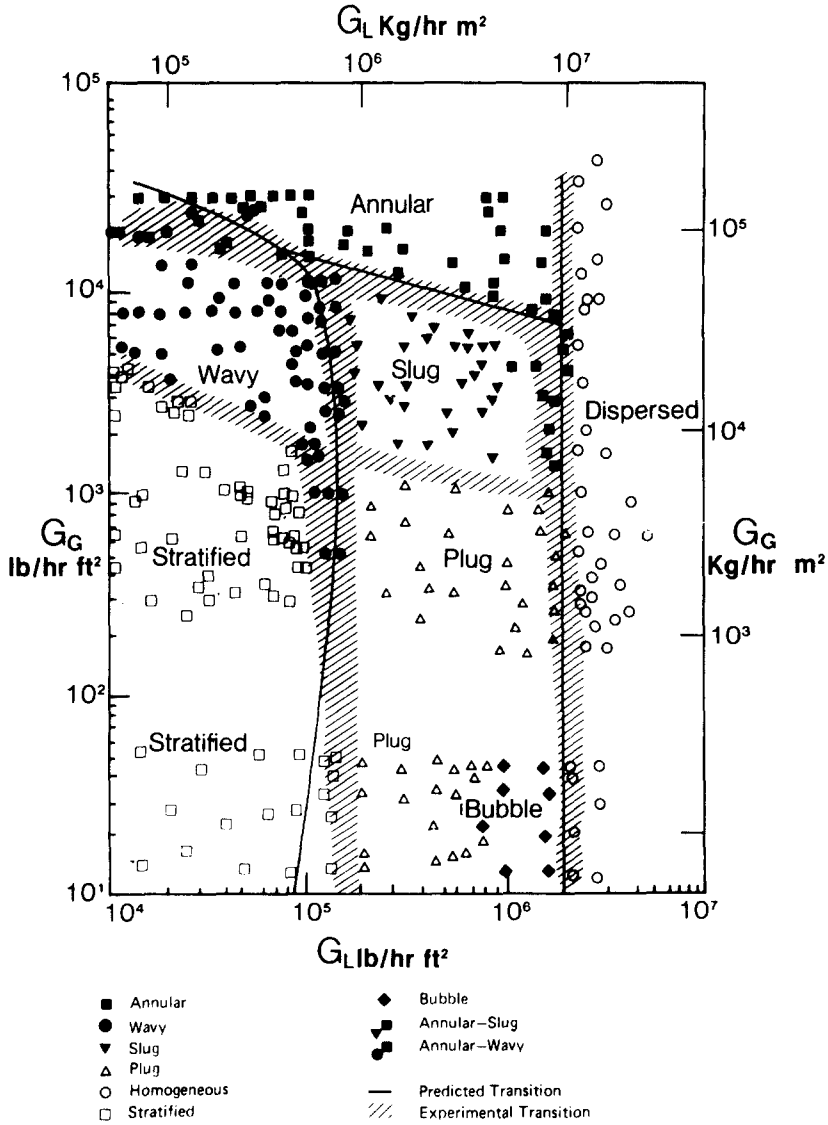

Figure 3(a). Flow pattern observations at end of 5.1 cm diameter line.

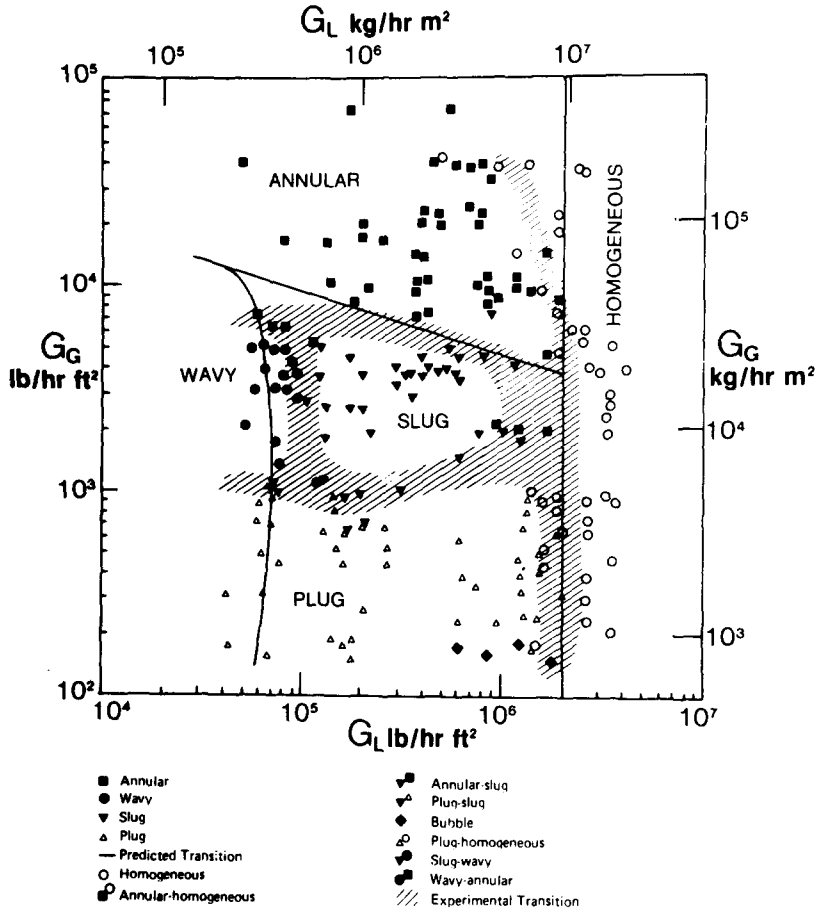

(b) Flow pattern observations at end of 1.2 cm diameter line.

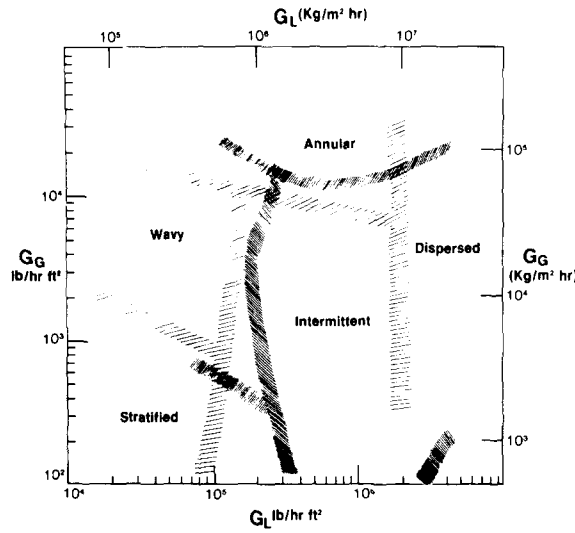

(c) Comparison of transitions in 2.54 and 12.7 cm lines.

Figure 3. Air-water flow patterns.

observations generally were in agreement with the concept that the entrance effect would depend on the ratio of distance from the mixer to the pipe diameter, (L/D). In the 1.15-cm line, the flow pattern maps at the three positions were essentially the same. In the 2.5-cm line, the transition from wavy to slug flow moved towards higher liquid flow rates at the entrance position. Differences between the middle and end position on the 2.5 cm line were very slight. At the entrance of the 5.1 cm line, the slug wavy transition was shifted to higher liquid ratio and the

transition to dispersed flow occurred at lower liquid flows. Differences in the observations at the middle and end of the 5.1 cm line were very small.

Based on the fact that in all lines the flow patterns were essentially unchanged from the middle to the end of the line, it was concluded that an adequate line length had been provided. It would appear that with the simple mixing device used here and in the absence of bends, an equilibrium situation is reached by $L/D \simeq 60$. When a mixing device in which the gas was introduced through a central annulus, was used, some changes between the middle and inlet positions in the 5.1-cm line could be observed in the transition from annular to slug flow. However, the transitions observed at the end of the 5.1-cm tube were identical to these seen with the simple mixing tee except for small changes in the slug-plug transition. This would appear to provide further assurance that the major flow pattern transitions (annular to separated and intermittent, intermittant and annular to dispersed, separated to intermittent) seen at the end position were not significantly influenced by inlet conditions.

For purposes of comparison with other fluids, the air–water data previously reported by Choe *et al.* (1978) for the end positions in 5.1 cm and 1.15 cm nominal lines are shown in figures 3(a) and 3(b). In these and subsequent maps, the individual symbols indicate the flow pattern observed at a particular set of gas and liquid flow rates. The shaded areas indicate the regions in which the flow pattern transition occurred. It will be observed that, in a given pipe line, the transition to dispersed flow occurs at a nearly constant liquid velocity. The transition occurs at a slightly lower liquid flow rate in the 1.15-cm tube. The transition between wavy and slug flow also appears to occur at a nearly constant liquid flow rate for a given pipeline diameter. Again the flow rate at which this occurs is reduced as the tube diameter is reduced. Annular flow occurs at high gas flow rates. The required gas flow for the transition increases with increasing tube diameter and decreasing liquid flow. It is interesting to note that, in going from slug to dispersed flow, annular flow is likely to be encountered. This narrow annular flow region was taken to be part of the unstable transition region since small changes in conditions led to the disappearance of the annular flow.

One may also note that at very low gas flows in the 5.1 cm tube, plug flow appears to be replaced by bubbly flow. In this region, the bubbles are not dispersed throughout the liquid but are found at the top of the pipeline.

The effect of pipeline diameter can be clearly seen from in figure 3(c) where the transition regions determined by Choe *et al.* (1978) for a 2.5 cm line are compared with the transition regions found for air–water in 12.7 cm lines by Simpson *et al.* (1977). Although the map of Simpson *et al.* is not complete, it is clear that the trends seen when comparing the 1.15 and 2.5-cm-dia. data are continued. Annular flow clearly begins at higher gas flow rates in the 12.7-cm line. Similarly, the intermittent and dispersed flow regions are shifted to higher liquid flow rates as the pipe diameter is increased.

USE OF PRESSURE DROP FLUCTUATIONS FOR FLOW PATTERN IDENTIFICATION

The use of completely visual observation for determining flow patterns has the disadvantage of being subjective. Differences in interpretation of visual observations are no doubt a major reason for experimenters having recorded different flow patterns under essentially similar conditions. The development of a simple quantitative means for distinguishing between flow patterns was therefore considered desirable.

Jones & Zuber (1974) have indicated that an analysis of the frequency spectrum of the output of a gamma densitometer can be used for distinguishing between flow patterns. Hubbard & Dukler (1966) showed that the analysis of the frequency of the fluctuations in pressure drop between two nearby wall locations may be similarly used. It was concluded that pressure drop fluctuations would furnish a very convenient means for flow pattern analysis. However, spectral analyses are complicated and facilities for such analyses are not universally available.

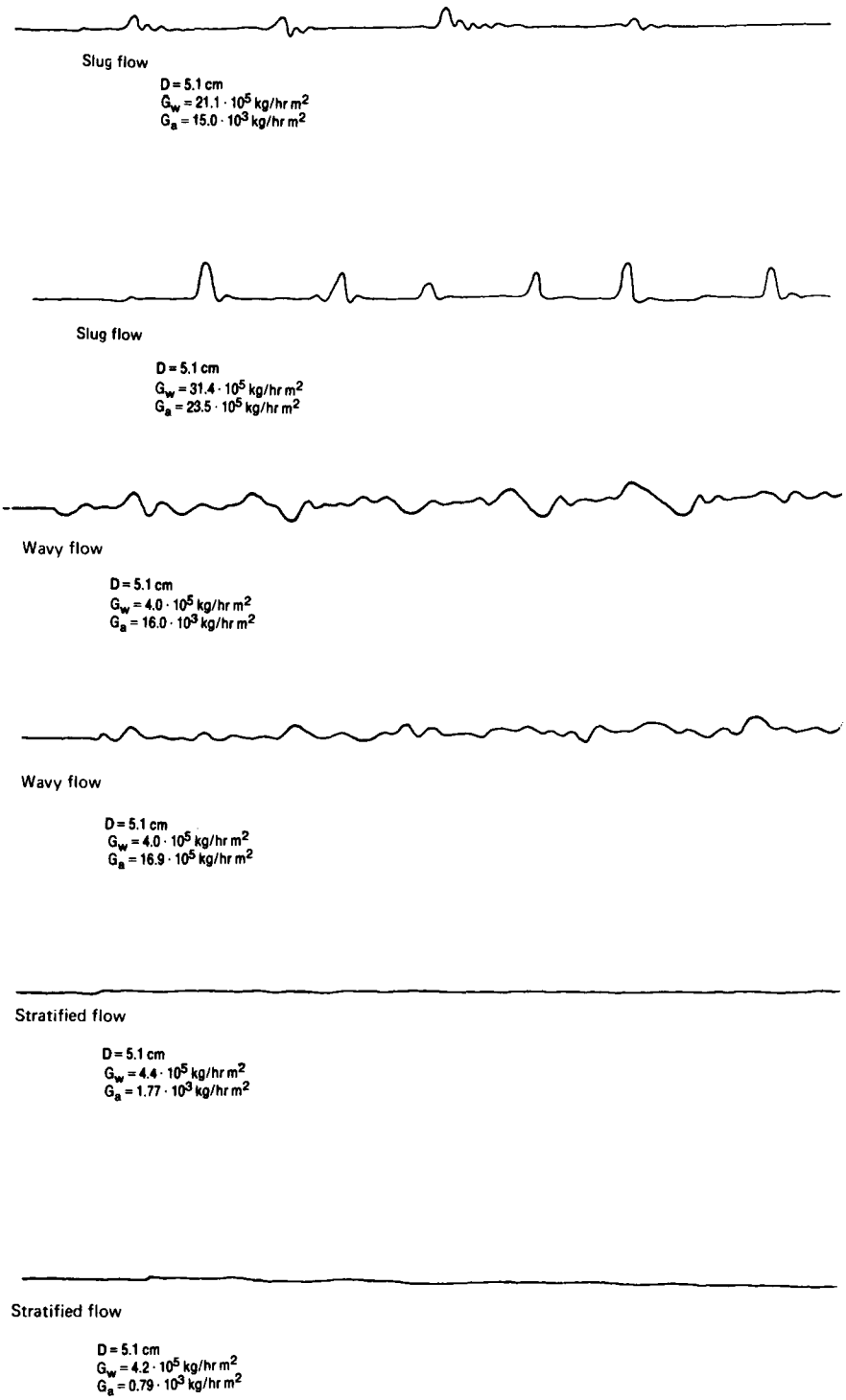

Figure 4. Pressure drop fluctuation traces for slug, stratified and wavy flow.

It was therefore decided to attempt to develop relatively simple criteria which could be readily applied to oscillograph traces of the pressure drop.

Slug flow had the most distinctive pressure traces. This region was characterized by a pressure drop trace with regularly spaced peaks. The quiescent regions between the peaks were at least twice the length (covered twice the time period) of the peaks. The distinctive slug flow pattern shown in figure 4(a) was reported previously by Choe *et al.* (1978) and used by them to establish the location of the slug-annular transition definitively.

Annular flow

$G_w = 7.4 \times 10^5$ kg/hr m^2
$G_a = 9.4 \times 10^4$ kg/hr m^2

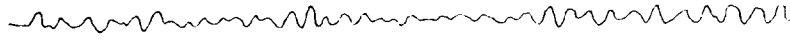

Annular flow

$G_w = 4.45 \times 10^5$ kg/hr m^2
$G_a = 10.8 \times 10^4$ kg/hr m^2

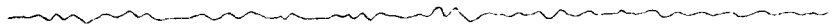

Wavy flow

$G_w = 35.2 \times 10^5$ kg/hr m^2
$G_a = 5.16 \times 10^4$ kg/hr m^2

Wavy flow

$G_w = 30.0 \times 10^5$ kg/hr m^2
$G_a = 5.16 \times 10^4$ kg/hr m^2

Dispersed flow

D = 5.1 mm
$G_w = 15.4 \times 10^5$ kg/hr m^2
$G_a = 16.4 \times 10^4$ kg/hr m^2

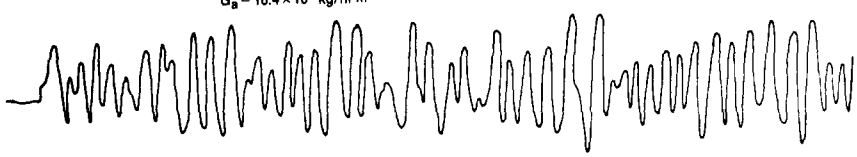

Dispersed flow

D = 5.1 cm
$G_w = 14.1 \times 10^5$ kg/hr m^2
$G_a = 5.6 \times 10^4$ kg/hr m^2

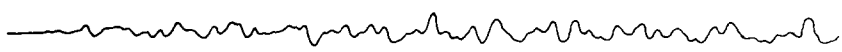

Annular flow

D = 5.1 cm
$G_w = 11.7 \times 10^5$ kg/hr m^2
$G_a = 6.5 \times 10^4$ kg/hr m^2

Annular flow

D = 5.1 cm
$G_w = 18.8 \times 10^5$ kg/hr m^2
$G_a = 13.6 \times 10^4$ kg/hr m^2

Figure 5. Pressure drop fluctuation traces for wavy, annular and dispersed flow.

As may be seen from the typical traces of figure 4(b), stratified flow shows essentially no fluctuations. It is readily distinguished from the clearly observable fluctuations of wavy flow. As the gas flow rate is increased, the frequency of the wavy flow fluctuations increases but their amplitude remains low (see figure 5a). When annular flow is observed, an increase in amplitude is observed (also see figure 5a). The transition between the two flow patterns may be determined from this change in amplitude.

The amplitude of the annular flow pressure drop fluctuations increases somewhat as we move towards higher liquid flows (see figure 5b). However, a further increase in amplitude is observed when we enter the dispersed flow region (see figure 5b). At high gas rates, the dispersed fluctuations have both a high frequency and amplitude. The transition between annular and dispersed flow can be most readily distinguished by considering the amplitude of the pressure fluctuations.

The amplitude of the dispersed flow fluctuations decreases as the gas rate is decreased (see figure 6). The frequency of the fluctuations remains high and thus frequency may be used to distinguish between the dispersed flow fluctuations and the low amplitude, low frequency plug flow fluctuations.

By comparison of figures 5 and 6, it will be seen that the pressure drop fluctuations produced by wavy and plug flow are very similar. Although the pressure drop fluctuation behavior does not permit any simple criterion for distinguishing between these flow patterns, this poses no difficulty since the two flow patterns are not adjacent in horizontal flow. Each of the required transitions can be distinguished in terms of fluctuation frequency, amplitude or, for the slug region, the pulse and quiescent region relationship.

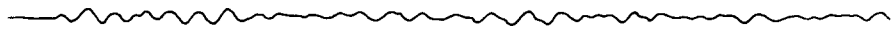

Plug flow

$D = 5.1$ cm
$G_w = 7.0 \times 10^6$ kg/hr m^2
$G_a = 2.1 \times 10^3$ kg/hr m^2

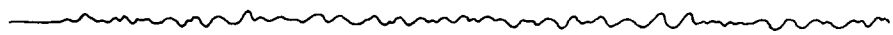

Plug flow

$D = 5.1$ cm
$G_w = 8.0 \times 10^6$ kg/hr m^2
$G_a = 2.2 \times 10^3$ kg/hr m^2

Dispersed flow

$D = 5.1$ cm
$G_2 = 6.6 \times 10^6$ kg/hr m^2
$G_a = 2.3 \times 10^3$ kg/hr m^2

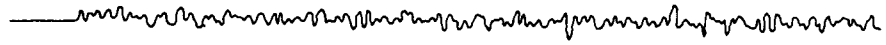

Dispersed flow

$D = 5.1$ cm
$G_w = 14.1 \times 10^6$ kg/hr m^2
$G_a = 3.5 \times 10^3$ kg/hr m^2

Figure 6. Pressure drop fluctuation traces for dispersed and plug flow.

Table 1. Criteria for determining flow patterns on basis of ΔP fluctuations

*Amplitude ratio = R, frequency = F.	Flow pattern	Range of applicability in horizontal air–water flow G_{water} $\frac{kg}{hr\text{-}m^2}$	G_{air} $\frac{kg}{hr\text{-}m^2}$
$R \geq 2.5$	Homogeneous	$5 \times 10^5 \leq G_w \leq 5 \times 10^7$	$3 \times 10^4 \leq G_a \leq 2 \times 10^5$
$R \leq 2.5$	Annular	$5 \times 10^5 \leq G_w \leq 5 \times 10^7$	$3 \times 10^4 \leq G_a \leq 2 \times 10^5$
Pressure fluctuation trace characterized by a pressure peak followed by a quiescent region whose length is at least twice the length of the peak	Slug	$5 \times 10^5 \leq G_w \leq 5 \times 10^6$	$5 \times 10^3 \leq G_a \leq 5 \times 10^4$
$R \geq 0.75$	Annular	$5 \times 10^4 \leq G_w \leq 5 \times 10^5$	$5 \times 10^4 \leq G_a$
$R \leq 0.75$ V 4 cycles/s	Wavy	$5 \times 10^6 \leq G_w \leq 5 \times 10^5$	$1.5 \times 10^4 \leq G_a \leq 5 \times 10^4$
$F \geq 7$ cycles/s	Homogeneous	$5 \times 10^6 \leq G_w \leq 5 \times 10^7$	$5 \times 10^2 \leq G_a \leq 5 \times 10^3$
$F \leq 6.5$ cycles/s	Plug	$5 \times 10^6 \leq G_w \leq 5 \times 10^7$	$5 \times 10^2 \leq G_a \leq 5 \times 10^3$
$R \geq 0.2$	Wavy	$5 \times 10^4 \leq G_w \leq 5 \times 10^5$	$1.5 \times 10^4 \leq G_a \leq 5 \times 10^4$
$R \leq 0.2$	Stratified	$5 \times 10^4 \leq G_w \leq 5 \times 10^5$	$5 \times 10^2 \leq G_a \leq 1.5 \times 10^4$

*Amplitude ratio based on the ratio of amplitude of the trace to the amplitude of the standard slug flow at fixed G_w and G_a:

$$G_w \simeq 1.1 \times 10^6 \text{ kg/h m}^2 \qquad G_a \simeq 1.5 \times 10^4 \text{ kg/h m}^2$$

After carefully examining the pressure drop fluctuation for water flow in horizontal tubes, the criteria shown in table 1 were established. It will be observed that the amplitude of the pressure fluctuations is expressed in terms of the ratio of the observed fluctuation of the fluctuation at a standard set of conditions.

The pressure drop fluctuation criteria of table 1 were used to establish flow pattern maps for air–water in horizontal flow. Comparison of these maps with those obtained visually showed very good agreement. The same procedure was subsequently followed for glycerine and salt solutions in horizontal flow. Again good agreement was obtained between flow maps based on visual observations and those obtained from application of the criteria of table 1 to the pressure drop fluctuations. In view of this agreement, the final flow maps prepared for the aqueous solutions used the pressure fluctuation data to supplement the visual observations. When visual observations were ambiguous, the pressure drop fluctuation data were used to identify the flow pattern.

EFFECTS OF LIQUID PROPERTIES ON FLOW PATTERN TRANSITIONS

To examine the effect of liquid viscosity on flow pattern transitions, a series of tests were carried out using glycerol–water solutions. Such solutions have the advantage of allowing liquid viscosity to be varied while holding surface tension nearly constant ($\sigma \simeq 65$ dyne/cm). In addition, the liquid density varies only slightly.

Two flow pattern maps were obtained in 5.1-cm horizontal lines for air–glycerol water solutions having a viscosity of 150 and 75 cp (figure 7 shows 75- and 150-cp data). The solution densities were 1.24 and 1.21 kg/l. High pressure drop prevented data from being obtained in smaller diameter lines.

The maps show relatively little change from the map obtained with water–air system, as far as the major flow patterns (separated, intermittent, dispersed) are concerned. The transition to dispersed flow is shifted to lower liquid flows (particularly at high gas rate) while the transition to annular flow appears to be shifted to slightly higher gas flow rates. Most of the former plug

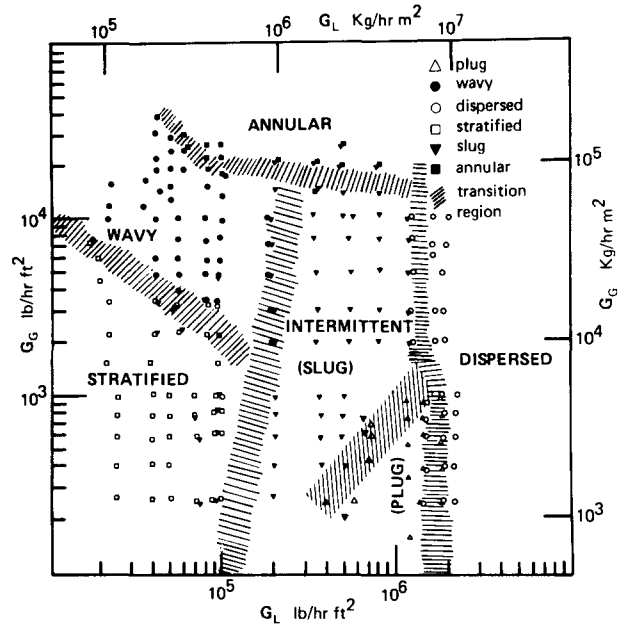

(a) 150 cp glycerine solution (ρ_L = 1.23 Kg/L σ = 65 dyne/cm).

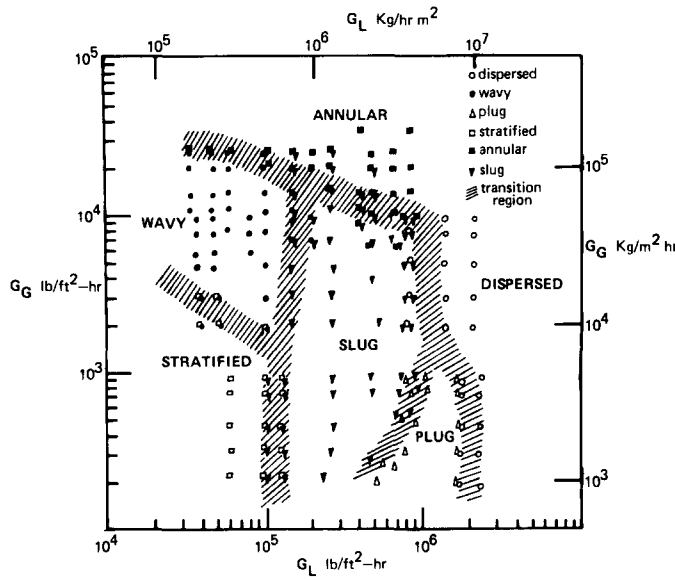

(b) 75 cp glycerine solution.

Figure 7. Flow pattern maps with high viscosity glycerine solutions.

flow region is now the slug flow area. The characteristic slug flow pressure drop was observed throughout the region indicated as slug flow and this confirmed the visual observations. It should be noted, however, that at the lowest gas rates the slugs were very slow moving and did not result in large pressure pulses. Although the slug flow region is generally avoided in industrial applications because of the possibility of equipment damage, the slow moving slugs seen at the low gas rates were no threat to system integrity.

To examine the effect of reducing the liquid surface tension, a surface active agent was added to the water thus decreasing the surface tension from about 68 to 38 dyne/cm.† Tests

†It is recognized that concentration of the surface active agent at the interface may have occurred and that simple surface tension measurements may not be a true indication of interface behavior. However, no simple organic dissolved in the water was found to show suitable surface tension lowering while being safe for laboratory use on a large scale. In view of the generally minor effects of surface tension, it is believed that the approach taken is justified.

with different surface active agents were carried out and Aliquat 221 (dimethyl, dialkyl ammonium chloride with alkyl portion of molecule derived from coconut oil fatty acids) produced by General Mills, which was less foamy than the others, was used.

The flow pattern maps in the 1.15-, 2.5- and 5.1-cm horizontal lines were determined. These data are shown in figure 8. Comparison of the observed transition regions with the dotted lines which indicate the behavior at $\sigma = 68$ dyne/cm, shows that the transition to annular and dispersed flow and the transition between intermittent and separated flow are essentially unchanged. The major change observed is that the wavy-stratified transition occurs at significantly higher gas flow rates.

The effect of liquid density (ρ_L) was examined next using potassium carbonate solution ($\rho_L = 1.42$ kg/l.). The viscosity was increased slightly to 3 cp and the surface tension was

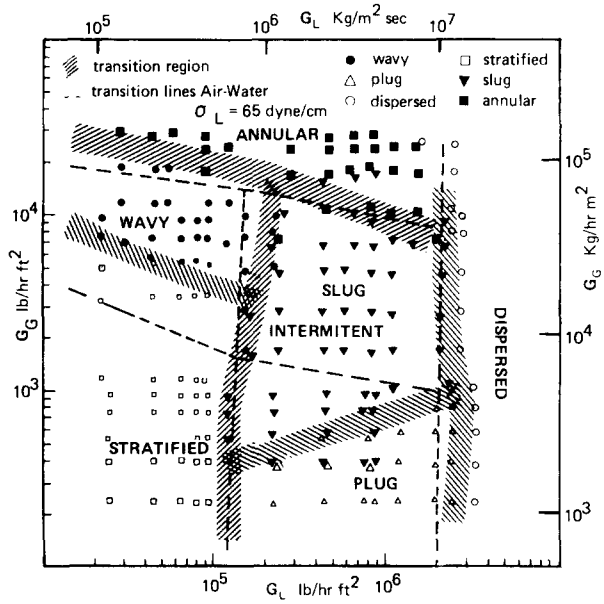

(a) 5.1 cm line.

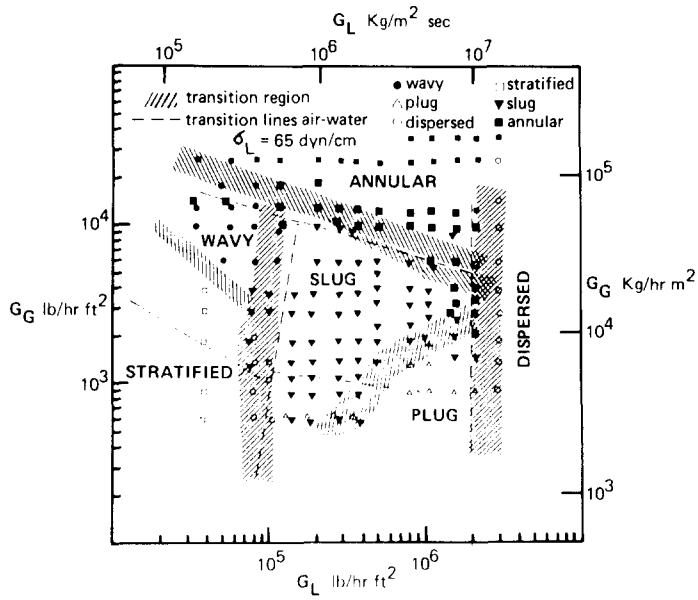

(b) 2.54 cm line.

Figure 8. Flow pattern maps for reduced interfacial tension test.

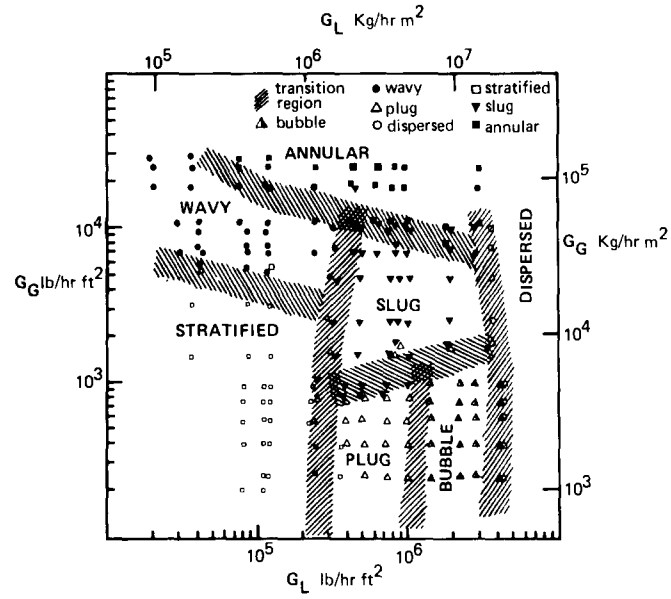

Figure 9. Flow pattern map for K_2CO_3 solution (ρ_L = 1.42 g/cm^3, μ_L = 3 cp, σ = 50 dyne/cm).

reduced slightly to 50 dyne/cm. In view of the small effect large viscosity changes had on the transition regions, and the observation that reducing surface tension by a factor of two did not significantly affect the major flow pattern transitions, it was concluded that the effects observed would be primarily due to the liquid density change.

Data were again obtained in the 2.5- and 5.1-cm lines and the results of the experiment in the 5.1-cm line are shown in figure 9. It is seen that transition to annular flow is essentially unchanged. The transition to dispersed flow and the transition from separated to intermittent flow are moved to higher liquid mass velocities. Note, that if the flow pattern map had been drawn in terms of superficial liquid velocities these transitions would have been virtually unchanged. The transition from stratified to wavy flow is, however, shifted to higher gas flow rates. In addition, the region of bubbly flow is considerably expanded.

EFFECTS OF VAPOR DENSITY

The final tests were conducted using the Freon 113–Freon 113 vapor system in the boiling loop previously described. These tests were conducted in order to evaluate the effect of vapor density. The experiments were run at ~1 bar and ~4 bars producing gas densities of 0.014 and 0.044 kg/l., respectfully (air in the air–water tests had density of approx. 0.0013 kg/l.). It should be observed that the density of liquid Freon 113 at these conditions is 1.45 and 1.35 kg/l., respectively. Viscosity has been reduced to about 0.3 centipoises and surface tension to about 13.5 dyne/cm at 1 bar and 9.5 dyne/cm at 4 bars.

The data obtained in the one inch glass line are shown in figures 10(a) and 10(b). If we compare these data to those obtained with the potassium carbonate solution (liquid density similar as density of K_2CO_3 solution in between those of the two Freon tests), we note little change in the transition to dispersed flow or the transition between separated and intermittent flow. The transition to annular flow occurs at much higher gas mass flow rates while the transition to wavy flow occurs at lower gas flow rates. (The gas mass flow rate, G_G, is clearly a poor correlating variable for the annular flow transition.) The transition between plug and slug flow is little changed but the large bubble flow region seen with the potassium carbonate solution is not seen here.

CORRELATION OF HORIZONTAL PIPELINE TRANSITION DATA

A wide variety of correlations have been proposed for flow pattern transitions in horizontal pipelines. One of the earliest and most widely used was that of Baker (1954) who proposed a

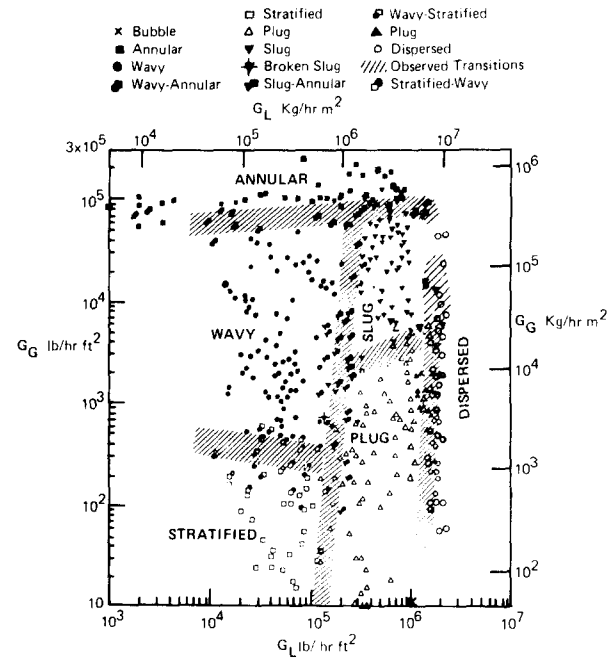

(a) P = 1 bar, D = 2.54 cm.

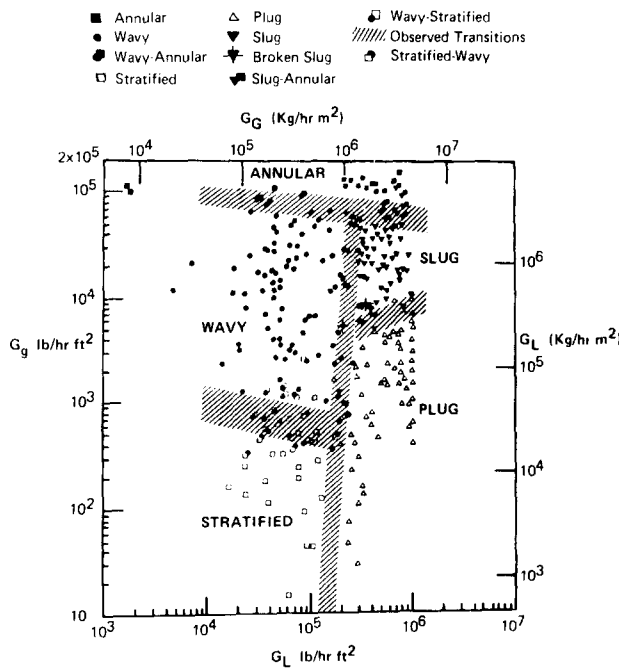

(b) P = 4 bar, D = 2.54 cm.

Figure 10. Flow patterns in Freon–Freon vapor systems.

flow-pattern map based on the coordinates G_L/λ and $G_L\,\lambda\psi/G_G$ where G_G, G_L = superficial gas and liquid mass velocities, respectivly; $\lambda = [(\rho_g/0.0012)(\rho_L/1.0)]^{1/2}$; $\psi = (73/\sigma)[\mu_L(1.0/\rho_L)^2]^{1/3}$; ρ_G, ρ_L = gas and liquid densities, respectively [kg/l.]; μ_L = liquid viscosity (centipoise); and σ = surface tension, (dyne/cm). More recently, the most widely used correlations appear to be those of Mandhane *et al.* (1974) or Taitel & Dukler (1976) Mandhane *et al.* used a map based on plotting V_{SL}, superficial liquid velocity, vs V_{sG}, superficial gas velocity. They concluded that any pipe diameter effects were small and hence only physical property corrections were

required to translate their air–water map to other systems. To use the map for other fluids the value of V_{sG} at which particular transition occurs is determined from the map for a given V_{SL}. A corrected value of the superficial gas velocity, V_{sG}^1, is then found from

$$V_{sG}^1 = f(x, y) \cdot V_{sG} \qquad [1]$$

where

$$x = \left[\left(\frac{\rho_G}{0.0013}\right)^{0.2}\left(\frac{\rho_L}{1.0}\frac{72.4}{\sigma}\right)^{0.25}\left(\frac{\mu_G}{0.018}\right)^{2}\right]$$

$$y = \left[\left(\frac{\mu_L}{1.0}\right)^{0.2}\left(\frac{\rho_L}{1.0}\frac{72.4}{\sigma}\right)^{0.25}\right] \qquad [2]$$

μ_G = gas viscosity (centipoise)

σ = interfacial tension (dyne/cm)

and f is specified for each transition and other quantities have their previous meaning. Note that the data from the present study and the large pipe size data of Simpson (1977) clearly show a pipe diameter effect which is not accounted for in the approach of Mandhane *et al.* (1974).

Taitel & Dukler (1976) attempted to develop a semi-theoretical base for their transition correlations. For horizontal pipelines, they expressed their results in terms of four dimensionless groups X, T, F and K. The dimensionless groups were defined by

$$X = \left(\frac{|(dp/dx)_L{}^S|}{|dp/dx)_G{}^S|}\right)^{1/2} \qquad [3]$$

$$T = \left(\frac{|(dp/dx)_L{}^S|}{(\rho_L - \rho_G)g\cos\theta}\right)^{1/2}$$

$$F = \sqrt{\left(\frac{\rho_G}{(\rho_L - \rho_G)}\right)}\frac{V_{SG}}{\sqrt{(Dg\cos\theta)}} = \frac{V_{SG}^*}{\sqrt{(\cos\theta)}}$$

$$K = F\left(\frac{DV_{SL}}{\nu_L}\right)^{1/2} = F(\mathrm{Re}_{SL})^{1/2}$$

where $(dp/dx)_G{}^s$, $(dp/dx)_L{}^s$ = pressure drop per unit length of gas and liquid flowing alone, respectively; D = pipe diameter; g = acceleration due to gravity; θ = angle of inclination; and ν_L = kinematic viscosity of liquid.

They concluded that the various transitions were controlled by the groupings tabulated below:

Stratified to annular—X, F.

Stratified to intermittent—X, F.

Intermittent to dispersed bubble—X, T.

Stratified smooth to stratified wavy—X, K.

Choe *et al.* (1978) carefully compared all of the major flow pattern transition correlations to the literature date available in 1975. In addition to the available air–water data he considered to non air–water data of Hoogendorn *et al.* (1959, 1961). He concluded that none of the published correlation schemes, including that of Taitel & Dukler (1976), were fully satisfactory. Choe *et al.* therefore developed a revised set of correlations which agreed with the data at his disposal.

Choe *et al.* found that Husain's (1975) simple correlation of the transition to dispersed flow was the most effective correlation for this flow pattern transition. This simple approach states that the flow is dispersed whenever

$$G_T = 1 \times 10^7 \text{ kg/h m}^2 \qquad [4]$$

and G_T = total mass flow rate of mixture.

For the transition between separated and intermittent flow, Choe *et al.* (1978) followed an approach similar to that used by Wallis & Dobson (1973). They were able to correlate the available data in terms of V_{sG}^* and α by the expression

$$V_{sG}^* = 2.5 \exp[-12(1-\alpha)] + 0.03\alpha \quad [5]$$

where $V_{sG}^* = (\rho_G^{1/2} V_{sG})/[gD(\rho_L - \rho_G]^{1/2}$ and α = void fraction, and other quantities are as previously defined. Although the data correlated by Choe *et al.* (1978) covered a number of liquids, the gas was air at near atmospheric pressure in all cases but one. The one exception was a test in which Freon vapor was used. The data for this test was above the line correlating the remaining air data and hence the predicted gas density effect could not be verified.

Choe *et al.* (1978) suggested that the transition to annular flow is due to periodic slugs or pulses which splashed liquid to the top of the tube. When the pulses are so frequent that the liquid is unable to drain before the next pulse or slug, annular flow begins. By using air–water slug frequency data, they concluded that the transition to annular flow can be correlated by the following dimensional equation

$$G_G = 1.3(G_L)^{-0.285}(D/D_c)^{0.38} \quad [6]$$

where D = pipe diameter (cm); D_c = standard pipe diameter of 3.05 cm; and G_G, G_L = mass velocity of gas and liquid, respectively (kg/m^2 h). Choe *et al.* concluded that much of the data found in the literature on the transition to annular flow was unreliable. They therefore compared their correlation only to the air–water transition data obtained at the University of Cincinnati.

The data from the present investigation taken together with that of Simpson *et al.* (1977) allow the various correlating approaches to be compared to a wider variety of fluids and a larger range of pipeline diameters. We shall follow Hubbard & Dukler's (1966) recommendation for the consolidation of the various flow patterns to annular, separated, intermittent and dispersed. The primary transitions considered will therefore be the transition to annular flow, transition to dispersed flow, and the transition between the separated and intermittent flow patterns.

Choe *et al.* (1978) showed that, for liquids of low or moderate viscosity, the Taitel–Dukler correlation between V_{sG}^* and X worked fairly well for the transition between separated and intermittent flow. However, when this correlation was applied to the data obtained with glycerine solutions very large discrepancies were observed (see figure 11). The Choe *et al.* correlation of V_{sG}^* vs α gave moderate agreement with the glycerine data when measured values of α were used. However, when a standard correlation such as that of Hughmark (1962) was used for estimating α for the glycerine data, wide discrepancies were observed. Since someone using such a relationship would have to rely on a α vs quality correlation, use of α as a

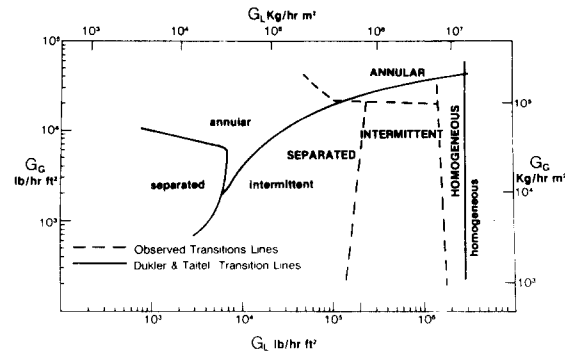

Figure 11. Comparison of Taitel–Dukler correlation with data for 150 cp glycerine solution.

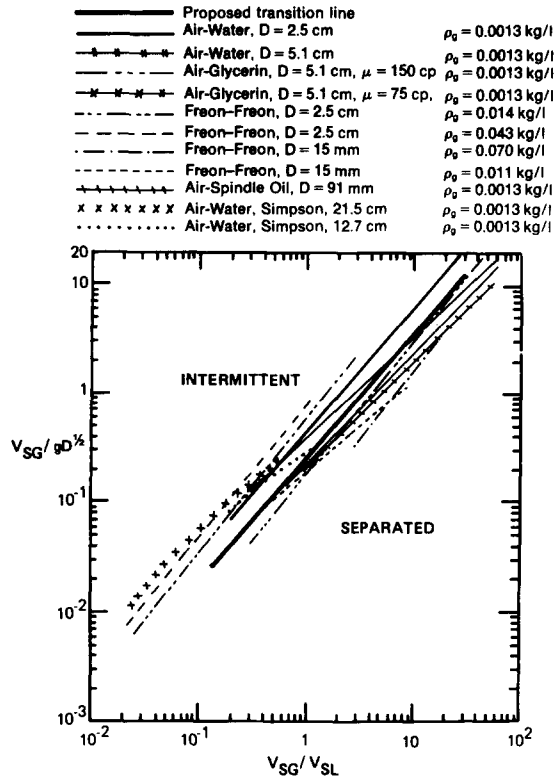

Figure 12. Separated-intermittent transition correlation.

correlating variable does not seem practical. By replacing α by the ratio (V_{sG}/V_{SL}), all of the data taken with air as the gas could be satisfactorily correlated against V^*_{sG}. However, the data obtained with Freon vapor did not show the predicted variation with vapor density. A very satisfactory correlation was obtained when the gas (Froude No.)$^{1/2}$ was used in place of V^*_{sG}. The final correlation proposed is

$$\frac{V_{sG}}{(gD)^{1/2}} = 0.25(V_{sG}/V_{SL})^{1.1}. \qquad [7]$$

It is compared to some of the experimental data in figure 12 where fairly good agreement is observed. Note that the correlation indicates that surface tension, liquid viscosity, and liquid density have no effect. This is in accord with the observations of the present tests.

Taitel & Dukler's (1976) correlation for the transition to annular flow is not as well grounded in theory as their other relationships. They simply proposed that the transition from intermittent to annular flow takes place when the ratio of equilibrium liquid level in the pipe, h_2, to pipe diameter exceeds 0.5. This assumption leads Taitel & Dukler to the conclusion that, in a plot of X vs F, the transition will take place at a constant value of X. The data reported by Choe *et al.* (1978) Simpson *et al.* (1977) and obtained in this investigation are in disagreement with this assumption. These data all indicate that the transition takes place more nearly at a constant value of F (figure 13). Since F and V^*_{sG} are identical for horizontal flow ($\cos\theta = 1$), the data are plotted in terms of V^*_{sG} vs (V_{sG}/V_{sL}) in figure 13(b). A fair agreement between the transition lines for the various fluids is obtained. It should be noted that this correlation procedure is essentially that proposed by Wallis (1968) for the annular flow transition in vertical lines. He suggested that one of the limits of the annular region is encountered when $V^*_{sG} = 0.9$. This is not very far from the region in which the transition occurs in horizontal lines.

The annular flow correlation shown in figure 13(b) appears to over-emphasize the effect of gas density. A somewhat improved correlation may be obtained by correlating the transition in

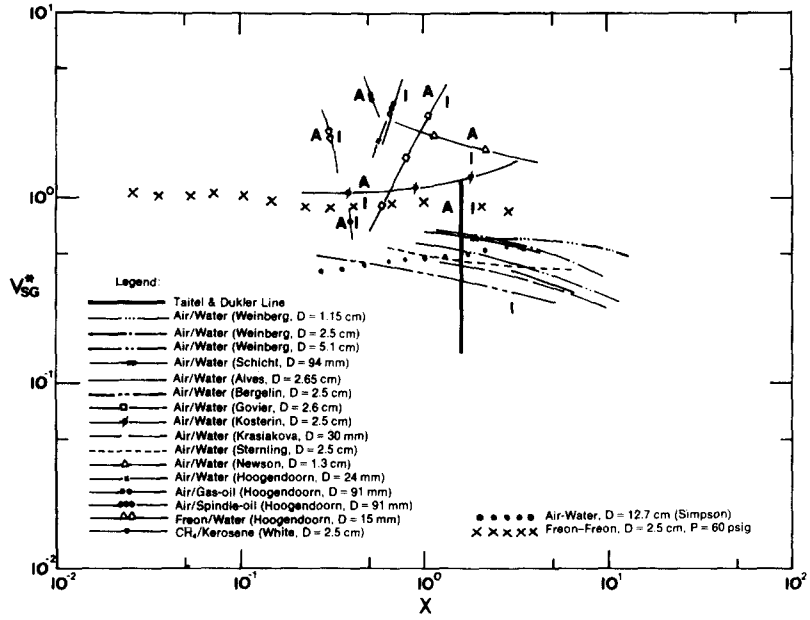

(a) Dukler–Taitel approach.

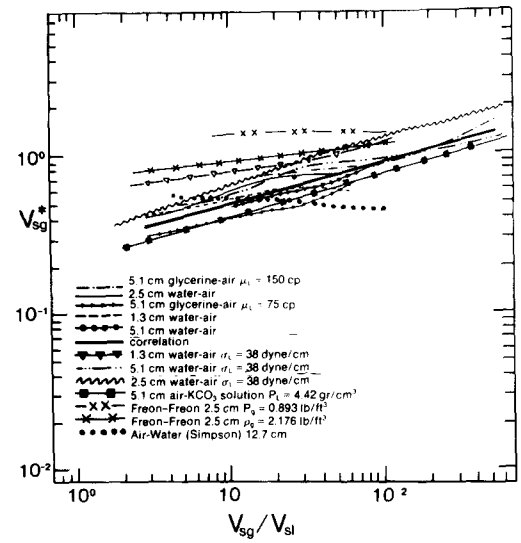

(b) Revised approach.

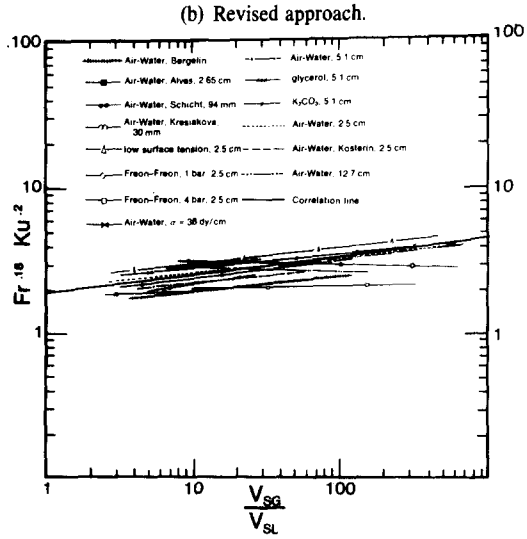

(c) Final approach.

Figure 13. Correlations to transition to annular flow.

terms of the Froude number, Fr, and the Kutdelaze number, Ku. This is illustrated in figure 18(c) where the data of this study and those of Simpson *et al.* (1977) are well fitted by

$$1.9(V_{sG}/V_{sL})^{1/8} = \mathrm{Ku}^{0.2}\mathrm{Fr}^{0.18} = \left(\frac{V_{sG}\rho_G^{1/2}}{[g(\rho_L-\rho_G)\sigma]^{1/4}}\right)^{0.2}\left(\frac{V_{sG}^2}{(gD)}\right)^{0.18}. \quad [8]$$

The correlation indicates no effect of liquid viscosity and very small effects for liquid density and surface tension which is in accord with the observations of the present tests.

Husain & Weisman (1978) and Taitel & Dukler (1976) have suggested that the transition to dispersed flow occurs when the turbulent fluctuations are sufficient to overcome the buoyant forces. The turbulent forces may be related to the pressure drop and hence Taitel & Dukler (1976) propose that the data be correlated in terms of a dimensionless ratio, T, which for horizontal lines is simply $[|(dp/dx)_L^s|/[\rho_L-\rho_G]g]^{1/2}$. The proposed correlation is compared to observed transition lines in figure 14(a). While the transition appears to take place in the range

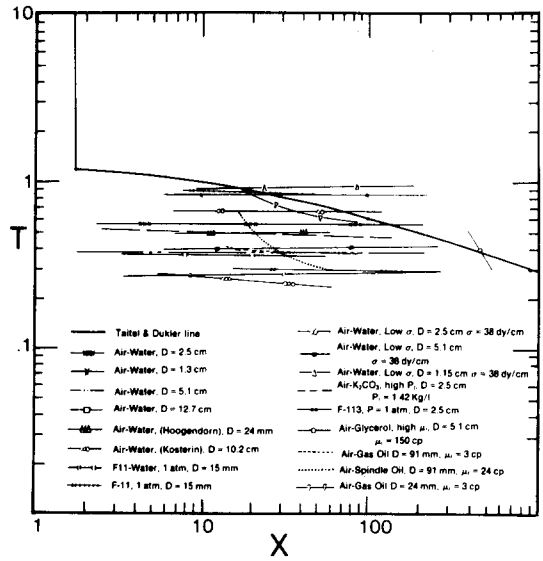

(a) Dukler-Taitel approach.

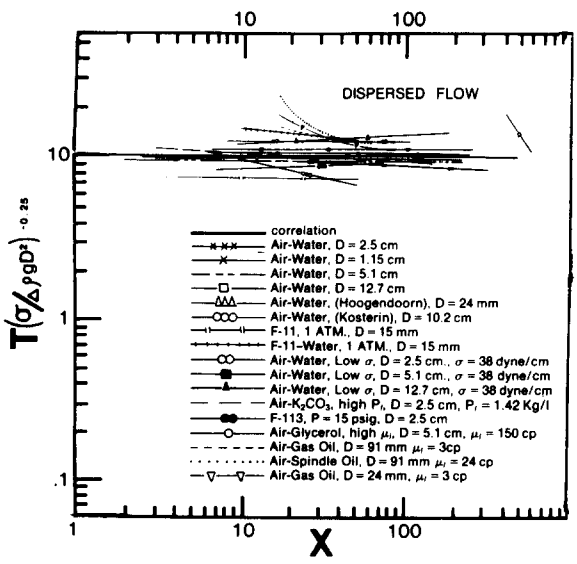

(b) Revised approach.

Figure 14. Dispersed flow transition correlations.

$0.2 \leq T \leq 0.9$, the effect of pipe diameter does not appear to be accounted for adequately. The correlation also fails to account for surface tension effects which, although small, were observable. An improved correlation of the data believed reliable is obtained by using the dimensionless group $[\sigma/(\Delta\rho g D^2)]$ to correct for surface tension and diameter effects (figure 14b). The horizontal data are reasonably well correlated by

$$\left[\frac{(dp/dx)_L}{\Delta\rho g}\right]^{1/2}\left(\frac{\sigma}{\Delta\rho D g^2}\right)^{-0.25} = 9.7 \qquad [9]$$

where $\Delta\rho = \rho_L - \rho_G$.

The effect of physical properties and pipe diameter are more easily seen if we note that for smooth tubes

$$(dp/dx)_L{}^S = \frac{f'}{2}\frac{G_L{}^2}{g_c\rho_L D} = c\left(\frac{DG_L}{\mu_L}\right)^{-0.2}\frac{G_L{}^2}{g_c\rho_L D} \qquad [10]$$

(with f' = friction factor) and recognize that for most conditions of interest $(\rho_L - \rho_G) \simeq \rho_L$. After some rearrangement, we obtain from the foregoing

$$G_L = c'(\rho_L{}^{0.83} D^{0.11}\sigma^{0.28}\mu_L{}^{-0.11}) \qquad [11]$$

where c' is a constant. We observe that the correlation predicts, that, for a given fluid and pipeline diameter, the transition to dispersed flow will occur at a constant liquid mass velocity. This is in generally good agreement with experimental observations and Husain (1975) and Choe *et al.*'s (1978) simplified correlation. Similarly, the experimental observations are not inconsistent with the predicted physical property effects. If we consider the behavior of the glycerine solutions, the viscosity effect is partially balanced by the density effect. The transition to dispersed flow is predicted to occur at about 70–75 per cent of the liquid mass velocity seen with water solutions. This appears to be in general accord with the data at high gas rates when the flow is certainly turbulent. At the lower gas flow rates, the higher liquid flows required are probably a reflection of the flows needed for the onset of turbulence. When Freon behavior is considered, the surface tension (for Freon 113 boiling at ~1 bar, $\sigma \simeq 13.5$ dyne/cm) and density effects counteract each other. This leads to the prediction that the transition occurs at nearly the same liquid flow rate as in the water–air system. This is in agreement with observations. The predicted effect of increased liquid density appears to be borne out by the potassium carbonate solution data. A predicted increase in G_L of about 40 per cent seems to be close to that observed.

Care should be used in using [9] at high qualities. The Taitel–Dukler derivation was devised for the dispersed bubble region only. Further, based on an analysis of frictional pressure drop data, Husain (1975) and Husain & Weisman (1978) concluded that at high qualities the homogeneous model fit the data when the total mass velocity was above about 1×10^7 kg/m^{2}h. They concluded that the flow pattern was probably dispersed (homogeneous) under these conditions. (Note that at low qualities, as in present tests, transition would occur when $G_L \simeq 1 \times 10^7$ kg/h^2.)

Husain & Weisman (1978) derived an alternative expression for the onset of dispersed flow which does lead to a transition criterion based on the total mass velocity, G_T, and which avoids introduction of an arbitrary dimensionless group. They argued that the theory developed for suspension of solid particles in pipelines (Weisman 1963) should apply to dispersion of bubbles providing the bubble rise velocity replaced the particle settling velocity. They concluded that at the onset of dispersed flow

$$\frac{P}{gv(\Delta\rho)u_b} = f(1-\alpha)\left(\frac{D}{d}\right)^n \qquad [12]$$

where P = power; u_b = bubble rise velocity; v = volume; and d = bubble diameter. They took the average bubble rise velocity as that proposed by Harmathy (1960)†

$$u_b = 1.53 g_c \left(\frac{g\Delta\rho\sigma}{\rho_L^2}\right)^{1/4}. \quad [13]$$

By noting that $P/v = \Delta p G_T / L\rho_{av}$ and assuming that the pressure drop, Δp, is given by homogeneous theory and $\rho_{av} \simeq (1-\alpha)\rho_L$ they obtained

$$(1-\alpha)f(1-\alpha)\left(\frac{D}{d}\right)^n = \frac{c\mu_L^{0.2}G^{2.8}}{2g_c D^{1.2}\rho_L^{1.75}g^{1/4}\sigma^{1/4}}. \quad [14]$$

The bubble diameter, d, was then taken as 45 per cent of the value suggested by Hinze (1955) for dispersed drops in another phase.‡ This gives

$$d = 0.725\left(\frac{\sigma}{\rho_L}\right)^{0.6}\left(\frac{P}{M}\right)^{-0.4}(g_c)^{0.2} \quad [15]$$

where M = mass, d = bubble diameter (cm).

Moderate agreement with the data was seen when $f(1-\alpha)$ and $(D/d)^n$ were taken as those found applicable to particle dispersion. It is more realistic to base these relationships on the available experimental observations for gas–liquid systems. If this is done, one would conclude $n = 0.8$ based on the observed diameter effect and $(1-\alpha)f'(1-\alpha)$ is near unity. After substitution of [15] for the particle diameter and rearranging we obtain

$$G_T = C(\rho_L^{0.51}D^{0.21}\sigma^{0.2}\mu_L^{-0.07}). \quad [16]$$

The similarities between [10] and [16] are obvious. Note that at low qualities, $G_L \simeq G_T$. The precision of the available low quality data is not sufficient to allow a clear choice between [11] and [16]. However, the general approach of [16] is supported by the recent work of Dalman & Hanratty (1978). They found that at very high qualities there is a gas flow rate above which a fully entrained condition is reached. At these high gas mass flow rates ($G_g \geq 0.85 \times 10^6$ kg/h m^2) the flow rate of the liquid on the wall film is very low (less than 2 per cent of total flow) and is independent of the liquid rate. If dispersed flow is defined as one in which entrainment exceeds 99.5 per cent, then it would begin at $G \simeq 0.35 \times 10^7$ kg/h m^2 in the air–water system in a 3.2-cm pipe.

The transition between the stratified and wavy flow patterns is not of major importance in horizontal flow since both pressure losses and mass transfer appear to be similar. However, once the pipeline is slightly inclined (upward) to the horizontal, stratified flow is replaced by plug flow and only wavy flow remains. A prediction of this behavior in horizontal flow is then needed as a base for future work in inclined lines.

The Taitel–Dukler (1976) correlation for this transition predicts a substantial effect of liquid viscosity which was not observed. Further, the experimentally observed surface tension effects are not predicted. Recent observations by Baryshev *et al.* (1978) with the air–water system in a rectangular duct indicate that the frequency of the waves tends to zero as the gas-phase

†For distorted flat drops the terminal settling velocity is given by [13] with the constant 1.53 replaced by 1.4. If the form of [15] is valid for d, then Husain & Weisman's approach would also hold for the transition to a dispersed flow of liquid drops in gas.

‡This assumption is generally consistent with the recent paper of O. Nagel entitled "Two-Phase Inter-Phase Phenomena in Chemical and Process Engineering" reported at the September 1978 Int. Seminar on Two-Phase Energy and Chemical Systems at Dubrovnik. Nagel concluded that gas bubble size in flowing fluids were proportional to $(P/\text{vol})^{-0.4}$.

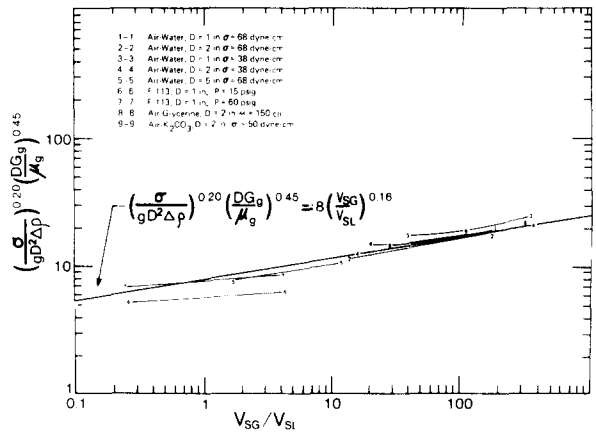

Figure 15. Wavy-stratified transition correlation.

Reynolds number is decreased. The gas phase Reynolds number, together with the group $(\sigma/gD^2\Delta\rho)$ introduced to account for surface tension and buoyancy effects, served as the major correlating variables. The final correlation obtained,

$$\left(\frac{\sigma}{gD^2\Delta\rho}\right)^{0.20}\left(\frac{DG_G}{\mu_G}\right)^{0.45} = 8(V_{sG}/V_{sL})^{0.16} \qquad [17]$$

is compared to the observed transition lines in figure 15.

OVERALL FLOW MAPS

The correlations proposed in [7]–[9] and [17] may be readily used to construct an overall flow map for a given fluid system and pipe diameter. This has been done for the air–water system in a 1 in. pipeline. In figure 16 the transition lines so obtained are plotted in terms of

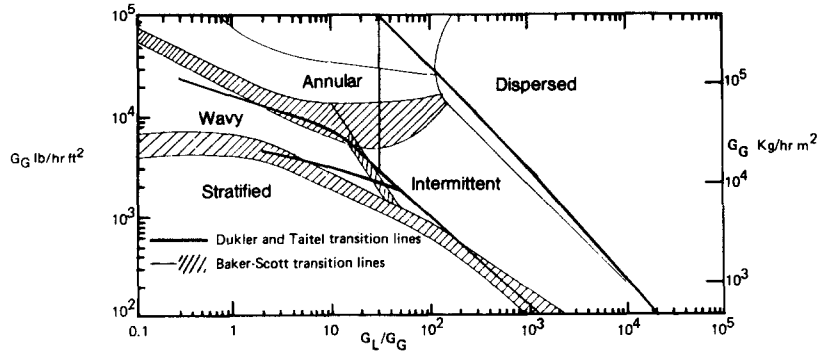

(a) Comparison of Dukler–Taitel and Baker–Scott maps.

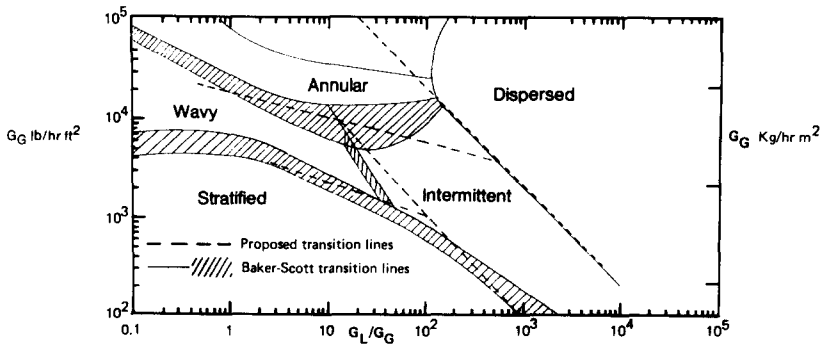

(b) Comparison of presently proposed map with Baker–Scott map.

Figure 16. Baker–Scott map compared to Taitel–Dukler and present transition correlations.

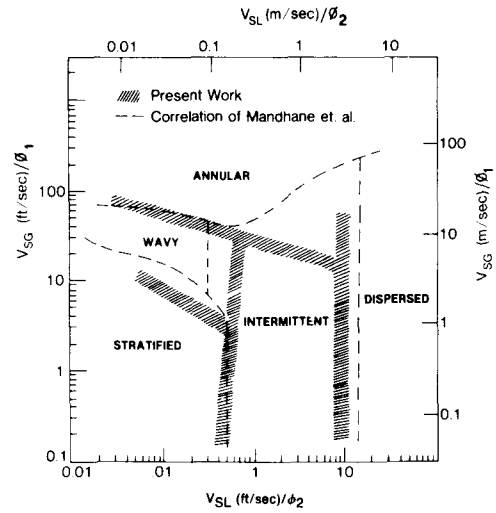

Figure 17. Overall flow pattern map (air-water, 1-in.-dia. line) for standard conditions.

Baker's (1954) coordinates and compared to the Baker-Scott (1963) transitions obtained from air-water data. It may be seen that there is generally good agreement. The Taitel-Dukler predictions are similarly plotted. For the air-water system, they also give generally good agreement except for the annular-intermittent transition which shows a decidedly different slope.

The presently proposed transition between intermittent and annular flow receives further support from Nguyen & Spedding's (1977) recent holdup studies. In these experimental studies of holdup in two-phase systems, they delineated three holdup regimes. Their regime II corresponds to the annular flow pattern. A boundary between this regime and others was determined from their air-water holdup data. The boundary so obtained corresponds closely with the transition line prediction of the present study for air-water in the same diameter line.

A flow map of general utility may be devised by recognizing that the major influences on flow patterns are the superficial gas and liquid velocities. This investigation has confirmed that both fluid properties and pipe diameter have only moderate influences. As suggested by Mandhane *et al.* (1974) an overall flow map in terms of V_{sG} and V_{sL}, may be devised if corrections are applied to the individual transition lines. Figure 17 presents such a map with the coordinates V_{sG}/ϕ_1 and V_{sL}/ϕ_2. For air-water at room conditions in a 2.54-cm-diameter line, ϕ_1 and ϕ_2 are 1.0. For other fluids and pipe diameters, the values of ϕ_1 and ϕ_2, which are derived from the proposed correlations, are obtained in accordance with table 2. For dispersed flow, the

Table 2. Property and pipe diameter corrections to overall flow map

	ϕ_1	ϕ_2
Transition to dispersed flow	1.0	$\left(\frac{\rho_L}{\rho_{sL}}\right)^{-0.33}\left(\frac{D}{D_s}\right)^{0.16}\left(\frac{\mu_{sL}}{\mu_L}\right)^{0.09}\left(\frac{\sigma}{\sigma_s}\right)^{0.24}$
Transition to annular flow	$\left(\frac{\rho_{sG}}{\rho_G}\right)^{0.23}\left(\frac{\Delta\rho}{\Delta\rho_s}\right)^{0.11}\left(\frac{\sigma}{\sigma_s}\right)^{0.11}\left(\frac{D}{D_s}\right)^{0.415}$	1.0
Intermittent-separated transition	1.0	$\left(\frac{D}{D_s}\right)^{0.45}$
Wavy-stratified transition	$\left(\frac{D_s}{D}\right)^{0.17}\left(\frac{\mu_G}{\mu_{sG}}\right)^{1.55}\left(\frac{\rho_{sG}}{\rho_G}\right)^{1.55}\left(\frac{\Delta\rho}{\Delta\rho_s}\right)^{0.69}\left(\frac{\sigma_s}{\sigma}\right)^{0.69}$	1.0

"s" denotes standard conditions

D_s = 1.0 in. = 2.54 cm $\quad\quad$ μ_{sl} = 1 centipoise

ρ_{sG} = 0.0013 kg/l. $\quad\quad$ σ_s = 70 dynes/cm

ρ_{sl} = 1.0 kg/l.

parameter exponents are an average of those obtained from [10] and [16]. Care should be taken not to extrapolate the dispersed flow correlation to higher qualities since the transition line shown does not reflect the idea that total mass flow rate controls the transition.

Although the transition from one flow pattern to another have been correlated as if the transition takes place suddenly along a single curve, this is not true in most cases. As may be seen from the various flow pattern maps presented in this paper, the transition from one pattern to another generally takes place over a range of conditions. In some transition regions, such as the transition from slug to dispersed flow, a third flow pattern (annular flow in the case cited) appears. The flow pattern map of figure 16 attempts to take this behavior into account by indicating the transitions as shaded regions of appropriate width. For comparison purposes, the transition lines of Mandhane *et al.* (1974) are also indicated on the figure. The comparison is generally good except for the annular-intermittent transition. It should be noted that the data available to Mandhane *et al.* was very scattered in this region.

CONCLUSIONS

The flow pattern data obtained in these tests together with the large pipe size data recently obtained by Simpson *et al.* (1977), provide a significantly improved basis on which to evaluate fluid property and pipe diameter effects. The new data show that the previously proposed correlations of Baker (1954) Taitel & Dukler (1976) Choe *et al.* (1978) and Mandhane *et al.* (1974) are not entirely satisfactory. Revised dimensionless correlations which agree with the new data and the reliable data in the literature have been devised.

These tests have confirmed that the major factor determining the flow pattern is the relative volumetric flow rates of gas and liquid. Following the format suggested by Mandhane *et al.* (1974), an overall flow pattern map has been developed in terms of V_{sG} and V_{sL}. The individual transition lines are corrected for fluid property and pipe diameter effects in accordance with the correlation governing the particular transition. It is believed that this map can be confidently used for flow pattern prediction.

NOMENCLATURE

d	particle or bubble diameter, L
$(dp \cdot dx)_G^s, (dp/dx)_L^s$	pressure drop per unit length due to gas or liquid, respectively, flowing alone, F/L^3
D	pipe diameter, L
f'	friction factor
g	acceleration due to gravity, L/T^2
G_g, G_L, G_T	gas, liquid and total mass flow rates, respectively based on superficial area, M/TL^2
L	pipe length, L
M	mass, M
p	pressure, F/L^2
P	power, FL/T
u_b	bubble rise velocity, L/T
v	volume
V_{sG}, V_{sL}	gas and liquid superficial velocities respectively, based on one phase flowing separately, L/T
V_{sG}^*	$(\rho_G^{1/2} V_{sG})[gD(\rho_L - \rho_G)]^{1/2}$
x	distance, L
α	void fraction
$\Delta\rho$	$(\rho_L - \rho_G)$
ν_L	kinematic viscosity of liquid, L^2/T
μ_G, μ_L	gas and liquid viscosities, M/LT

ρ_G, ρ_L gas and liquid densities, respectively, M/L^3
σ interfacial tension, F/L
θ angle of inclination

REFERENCES

ALVES, G. E. 1954 Concurrent liquid–gas flow in a pipeline contactor. *Chem. Engng Prog.* **50**, 449–456.

BAKER, O. 1954 Speed-up flow calculations for design of gas gathering systems. *Oil and Gas J.* **53**(12), 185–190.

BARYSHEV, Y., BESFAMIBLYE, P. & TSIKAURIE, G. 1978 Experimental investigation of hydrodynamical processes in the wavy interface of liquid and air flows. *Proc. Int. Seminar on Momentum Heat and Mass Transfer—Two-Phase Energy and Chemical Systems*, Dubrovnik, Yugoslavia.

BERGELIN, O. P. & GAZLEY, G. 1949 Co-current gas–liquid flow in horizontal tubes. *Proc. Heat Transfer and Fluid Mechanics Institute*, Stanford University.

CHOE, W. G., WEINBERG, L. & WEISMAN, J. 1978 Observation and correlation of flow pattern transition in horizontal, co-current gas–liquid flow. In *Two-Phase Transport and Reactor Safety* (Edited by VEZIROGLU T. N. & KAKAC S.). Hemisphere, Washington.

DOLMAN, J. C. & HANRATTY, T. J. 1978 Interpretation of entrainment measurements in annular gas–liquid flows. *Proc. Int. Seminar on Momentum and Mass Transfer—Two-Phase Energy and Chemical Systems*, Dubrovnik, Yugoslavia.

EATON, B. A., ANDREWS, D. E., KNOWLES, C. R., SILBERBERG, I. H. & BROWN, K. E. 1967 The Prediction of flow patterns, liquid holdup and pressure losses occurring during continuous two-phase flow in horizontal pipeline. *J. Petrol Tech.* **19**, 815–828.

GOVIER, G. W. & OMER, M. M. 1962 The horizintal flow of air-water mixtures. *Can. J. of Chem. Engng* **40**, 93–104.

HARMATHY, G. A. 1960 Velocity of large drops and bubbles in media of infinite or restricted extent. *A.I.Ch.E.J.* **6**, 281–288.

HINZE, J. O. 1955 Fundamentals of the hydrodynamic mechanism of splitting in dispersion processes. *A.I.Ch.E.J.* **1**, 289–295.

HOOGENDORN, C. J. 1959 Gas–liquid flow in horizontal pipes. *Chem. Engng Sci.* **9**, 205.

HOOGENDORN, C. J. & BEUTELAAR, A. A. 1961 Effects of gas density and gradual vaporization on gas-liquid flow in horizontal lines. *Chem. Engng Sci.* **16**, 208–215.

HUBBARD, M. G. & DUKLER, A. E. 1966 The characterization of flow regimes in horizontal two-phase flow. *Proc. Heat Transfer and Fluid Mechanics Inst.*, Stanford University.

HUGHMARK, G. A. 1962 Hold-up in a gas–liquid flow. *Chem. Engng Prog.* **55**(4), 62–65.

HUSAIN, A. 1975 Applicability of homogeneous model to two-phase flow. Ph.D. Thesis, University of Cincinnati.

HUSAIN, A. & WEISMAN, J. 1978 Applicability of homogeneous flow model to two-phase pressure drop in straight pipe and across area changes. *A.I.Ch.E. Symp. Series* 174 **74**, 205–214.

JONES, O. & ZUBER, Z. 1974 Statistical methods for measurement and analyses of two-phase flow. *Proc. Int. Heat Transfer Conf.*, Tokyo, Japan.

KOSTERIN, S. I. 1949 An investigation of the influence of diameter and inclination of a tube on the hydraulic resistance and flow structure in gas–liquid mixtures. *Izvestia Akademe Nauk., USSR, O.T.N.* **12**, 1824.

MANDHANE, J. M., GREGORY, G. A. & AZIZ, K. A. 1974 A flow pattern map for gas–liquid flow in horizontal pipeline. *Int. J. Multiphase Flow* **1**, 537–554.

NGUYEN, V. T. & SPEDDING, P. L. 1977 Hold-up in two-phase gas–liquid flow. *Chem. Engng Sci.* **32**, 1003–1021.

SAKUGACHI, K., AKAGAWA. K., HAMAGUCHI, H. & ASHIWAKE, N. 1973 Transient behavior of air–water two-phase flow in a horizontal tube. ASME Paper 73-WA/H7-21.

SCHICHT, H. H. 1969 Flow patterns for adiabatic two-phase flow of water and air within a horizontal tube. *Verfahrenstecknik* **3**, 153–172.

SCOTT D. S. 1963 Properties of co-current gas–liquid flow. In *Advances in Chemical Engineering*, Vol. 4. Academic Press, New York.

SIMPSON, H. C., ROONEY, D. H., GRATTON, E. & AL-SAMARRAL, F. 1977 Two-phase flow in large diameter horizontal lines. Paper H6, European Two-Phase Flow Group Meeting, Grenoble.

TAITEL, Y. & DUKLER, A. E. 1976 A model for predicting flow regime transitions in horizontal and near-horizontal flow. *A.I.Ch.E.J.* **22**, 47–55.

WALLIS, G. B. 1968 Vertical annular flow—a simple theory. Paper presented at AIChE Annual Meeting, Tampa, Florida.

WALLIS, G. B. & DOBSON, J. E. 1973 The onset of slugging in horizontal, stratified air–water flow. *Int. J. Multiphase Flow* **1**, 173–193.

WEISMAN, J. 1977 Experimental data on two-phase ΔP across area changes during transients. U.S. Nuclear Energy Commission Rep. NUREG-0306.

WEISMAN, J. 1963 Minimum power requirements for slurry transport. *A.I.Ch.E.J.* **9**, 134–138.

WHITE, P. D. & HUNTINGTON, P. 1955 Horizontal co-current two-phase flow of fluid in pipe lines. *Petroleum Engng* **27**(9), D40.